IAI Journals.ASM.org

Uptake and Persistence of *Mycobacterium avium* subsp. *paratuberculosis* in Human Monocytes

Dayle A. Keown,[a,b] David A. Collings,[b] and Jacqueline I. Keenan[a]

Department of Surgery, University of Otago Christchurch, Christchurch, New Zealand,[a] and School of Biological Sciences, University of Canterbury, Christchurch, New Zealand[b]

***Mycobacterium avium* subsp. *paratuberculosis* is a bacterium sometimes found in human blood and tissue samples that may have a role in the etiology of Crohn's disease in humans. To date, however, there have been few studies examining the interactions of these bacteria with human cells. Using the THP-1 human monocytic cell line, this study shows that the uptake and trafficking of *M. avium* subsp. *paratuberculosis* in human cells are cholesterol dependent and that these bacteria localize to cholesterol-rich compartments that are slow to acidify. *M. avium* subsp. *paratuberculosis* bacteria containing phagosomes stain for the late endosomal marker Rab7, but recruitment of the Rab7-interacting lysosomal protein that regulates the fusion of bacterium-containing phagosomes with lysosomal compartments and facilitates subsequent bacterial clearance is significantly reduced. Disruption of phagosome acidification via this mechanism may contribute to *M. avium* subsp. *paratuberculosis* persistence in human cells, but there was no evidence that internalized *M. avium* subsp. *paratuberculosis* also affects the survival of bacteria taken up during a secondary phagocytic event.**

Mycobacterium avium subsp. *paratuberculosis* is a bacterium that causes chronic enteritis in domestic and wild ruminants and other animals, including primates (35). The similarities between the gross pathology and histology of *M. avium* subsp. *paratuberculosis*-related disease in animals and Crohn's disease (CD) in humans (17) have led to the suggestion that *M. avium* subsp. *paratuberculosis* may also have a role in the etiology of the latter. CD is a chronic inflammatory disease of the human gastrointestinal tract that is characterized by weight loss, severe diarrhea, and abdominal pain (5). Several further observations strengthen this hypothesis: the detection of the specific DNA insertion sequence IS*900* of *M. avium* subsp. *paratuberculosis* in relatively high numbers in the blood and tissues of patients with CD (1, 2), the finding of *M. avium* subsp. *paratuberculosis*-reactive T cells in CD patients (29), and the culture of viable *M. avium* subsp. *paratuberculosis* forms from blood of people with CD (28).

In infected animals, *M. avium* subsp. *paratuberculosis* enters the body via the fecal-oral route, moves across the intestinal epithelium, and then uses complement-associated and non-complement-associated receptors to gain entry to host phagocytic cells (36, 44), where it is able to persist by inhibiting phagosome-lysosome function (4, 23, 43). Mannosylated lipoarabinomannan (Man-LAM), a major component of the *M. avium* subsp. *paratuberculosis* cell wall, contributes to this via Toll-like receptor 2 (TLR2) signaling and activation of the *M. avium* subsp. *paratuberculosis* K-p38 signaling pathway (37, 42) that has been shown to block phagosomal acidification by signaling across the phagosome wall (11). However, additional pathways may also be involved in *M. avium* subsp. *paratuberculosis* survival, as has been reported for pathogenic mycobacteria such as *M. tuberculosis* and *M. bovis*. These species have been reported to use receptor-mediated association with cholesterol-rich areas of the plasma membrane (22) to enter cells and traffic to cholesterol-rich compartments (12), where they persist by utilizing host cholesterol (30) and blocking normal phagosome maturation. This is demonstrated by reduced fusion of bacterium-containing phagosomes with lysosomes (6) and the absence of RILP (Rab7-interacting lysosomal protein) in Rab7-staining phagosomes that contain live mycobacteria (38). However, it is unclear whether it is the cholesterol-rich membranes (7, 20) and/or factors secreted by the mycobacteria themselves (38, 39) that dictate this lack of fusion.

The aim of our study was to investigate the uptake and survival of *M. avium* subsp. *paratuberculosis* in human cells. Using the THP-1 human monocyte cell line, we observed that *M. avium* subsp. *paratuberculosis* enters cells at regions enriched for cholesterol and remains associated with cholesterol-rich areas of the cell to 48 h postinfection in compartments that show evidence for reduced acidity. Intriguingly, the compartments containing live *M. avium* subsp. *paratuberculosis* also showed evidence of reduced recruitment of RILP, despite the presence of Rab7, indicating the potential expression of a Rab7-deactivating factor by *M. avium* subsp. *paratuberculosis*. We hypothesized that diffusion of such a deactivating factor by *M. avium* subsp. *paratuberculosis* might confer an intracellular survival advantage to other phagocytosed bacteria, as described for *M. bovis* (38). However, we found no evidence that live *M. avium* subsp. *paratuberculosis* inside monocytes decreased the killing efficiency of cells presented with a second bacterial challenge.

MATERIALS AND METHODS

Reagents and antibodies. CDP-Star substrate, fluorescein isothiocyanate (FITC), LysoTracker Red, filipin, Texas Red-conjugated phalloidin, and Hoechst stain were purchased from Invitrogen (Carlsbad, CA). The pro-

Received 21 May 2012 Returned for modification 27 June 2012
Accepted 1 August 2012
Published ahead of print 13 August 2012
Editor: J. L. Flynn
Address correspondence to Jacqueline Keenan, jacqui.keenan@otago.ac.nz.
Supplemental material for this article may be found at http://iai.asm.org/.

doi:10.1128/IAI.00534-12

tease inhibitor cocktail and the enzymatic colorimetric reagent for measuring cholesterol (CHOD-PAP) were from Roche (Manheim, Germany), gentamicin was from Pfizer (Bentley, WA, Australia), and simvastatin and methyl-β-cyclodextrin (MβCD) were from Sigma (St. Louis, MO). Rabbit polyclonal antibodies to Rab5a, Rab7, and RILP were purchased from Santa Cruz Biotechnology (Santa Cruz, CA), whereas the secondary antibodies were from Invitrogen.

Bacteria. *M. avium* subsp. *paratuberculosis* strain Dominic (ATCC 43545) and *M. bovis* (ATCC 19210) were grown in Middlebrook 7H9 broth (Becton Dickinson, Sparks, MD) supplemented with oleic acid-albumin-dextrose-catalase (Becton Dickinson), 0.05% Tween 80, and 2 μg/ml mycobactin J (Allied Monitor, Fayette, MO) at 37°C on a rotating platform (100 rpm). *Escherichia coli* strains BL21 (ATCC BAA-1025) and LF 82 (kindly provided by A. Darfeuille-Michaud, Laboratoire de Bactériologie, CBRV, Clermont-Ferrand, France) were grown overnight in brucella broth (Becton Dickinson) under the same conditions. Bacteria were harvested in mid-log phase and quantitated using the method of Glubb et al. (16). Control bacteria were killed by heating at 95°C for 15 min. Direct FITC labeling (final concentration, 100 μg/ml) was at 37°C for 1 h, with unbound dye removed by extensive washing with phosphate-buffered saline (PBS; 137 mM NaCl, 2.7 mM KCl, 4.3 mM Na_2HPO_4, 1.47 mM KH_2PO_4) (14). Mycobacterial preparations were briefly sonicated (Omni-Ruptor 4000 sonicator) prior to infection to disperse clumps. The multiplicity of infection (MOI) for each experiment was 50:1, unless stated otherwise.

Cell culture. The human monocytic THP-1 cell line (ATCC TIB-202) was grown in RPMI 1640 (Gibco, Invitrogen, Auckland, New Zealand) containing 10% heat-inactivated fetal bovine serum (FBS), 1% penicillin-streptomycin, and 1% GlutaMAX supplement (all from Gibco). Purified human monocytes were obtained by immunomagnetic positive selection of CD14-positive cells from the peripheral blood mononuclear cell (PBMC) layer of fresh blood following density gradient centrifugation, as detailed by the manufacturer (Miltenyi Biotec, Bergisch Gladbach, Germany), resuspended in the same medium, and cultured overnight prior to use. Cell culture was at 37°C in air containing 5% CO_2.

Fluorescence microscopy. Cells were cytospun onto coverslips (400 rpm, 5 min), fixed using 4% (vol/vol) formaldehyde (in PBS), and formaldehyde-induced autofluorescence quenched (1.5 mg/ml glycine in PBS, 10 min). Where immunofluorescence microscopy was used, cells were then permeabilized (0.1% Triton X-100 in PBS, 10 min) and blocked with 5% (vol/vol) FBS (in PBS) for 60 min at 37°C before overnight incubation at 4°C in primary antibody (1:1,000 dilution in PBS containing 2.5% FBS), followed by a Texas Red-conjugated chicken anti-rabbit secondary antibody for 4 h at room temperature (1:500 dilution in PBS containing 2.5% FBS). After two washes (PBS, 0.1% Triton X-100), cell nuclei were stained with Hoechst (0.25 μg/ml in PBS containing 2.5% FBS) at 37°C for 5 min and then washed once more. The cells were mounted with 0.1% (wt/vol) *p*-phenylenediamine dihydrochloride and examined using epifluorescence microscopy on an AxioImager Z1 upright microscope with a ×40 plan Neofluar lens (Zeiss, Oberkochen, Germany). Images were taken at the same exposure for each replicate with an Axiocam MRm camera coupled to Axiovision software.

For cholesterol colocalization experiments, the cells were incubated with filipin (100 μg/ml) and Texas Red-phalloidin (1 U/ml) for 30 min at 37°C, washed, and mounted. Filipin was visualized with excitation (360 nm) and emission (405 nm) through a standard UV filter block, while Texas Red was viewed with excitation (591 nm) and emission (608 nm) and photographed as described above.

Acidified compartments were identified by preloading THP-1 cells (2×10^5) with 100 nM LysoTracker Red (in medium) for 2 h at 37°C prior to infection (40). After uningested bacteria were removed, cells in each well were resuspended in 100 nM LysoTracker Red to ensure effective labeling of acidic compartments. At 2 and 48 h postinfection, the cells were washed, fixed, and mounted, and the percentage of FITC-fluorescing phagosomes colocalizing with LysoTracker Red was determined manually by counting cells strongly, weakly, or not stained with LysoTracker Red.

Cholesterol depletion. THP-1 cells were incubated with simvastatin (final concentration, 2.5 μg/ml) for 48 h and then resuspended at a concentration of 2×10^5 cells/ml in MβCD for 1 h before the addition of FITC-labeled bacteria (MOI, 50:1) for 4 h. The washed cells were lysed (20 mM HEPES at pH 7.5, 0.35 M NaCl, 20% glycerol, 1% NP-40, 1 mM $MgCl_2$, 0.5 mM EDTA, 0.1 mM EGTA, and protease inhibitor cocktail), and an equal volume of lysate was added to CHOD-PAP reagent, followed by spectrophotometric measurement at 490 nm. The cholesterol content of cells was expressed as micrograms of cholesterol per milligram of cellular protein (34).

Flow cytometry. Cells were resuspended in 5% (vol/vol) FBS in PBS containing 5 μg/ml propidium iodide (PI), and fluorescence measurements were made using a flow cytometer (Cytomics FC 500 MPL; Beckman Coulter) and CXP software (Beckman Coulter). Ten thousand events were collected for each sample, with dead cells excluded by positive PI staining and size stratification used to exclude remaining nonadherent bacteria. Mean fluorescence intensity (MFI) values of cells incubated in the absence of bacteria were subtracted from the values of bacterium-treated cells. To determine the proportion of internalized bacteria, fluorescence was measured before and after the addition of trypan blue (final concentration, 0.025%) to quench extracellular bacterial fluorescence (45).

Phagosome extraction and immunoblotting. THP-1 cells (2×10^6) were infected (MOI, 50:1) for 1 or 2 h, washed, and chased for 2 or 48 h (in medium), before being lysed by sonication (in 250 mM sucrose, 0.5 mM EGTA, 20 mM HEPES-KOH, pH 7.2). Unbroken cells and whole nuclei were removed (2,000 rpm at 4°C for 3 min) before the lysates were centrifuged through a sucrose density gradient (65% to 10%) at 100,000 × *g* for 1 h at 4°C. Phagosome-rich fractions (26) were transferred onto a polyvinylidene difluoride (PVDF) membrane (Bio-Rad, Hercules, CA) and probed with an anti-RILP antibody (final concentration, 10 μg/ml diluted in 2.5% nonfat milk blocking buffer), followed by an alkaline phosphatase-conjugated secondary antibody (1:10,000 dilution in 2.5% nonfat milk blocking buffer). The membrane was developed with chemiluminescent substrate (CDP-Star; New England BioLabs, Ipswich, MA), and the signal was visualized using a Chemidoc XRS system (Bio-Rad). After stripping (0.1 M glycine-HCl, pH 2.5) for 1 h at 37°C, three 5-min Tris-buffered saline–0.05% Tween 20 (TBS-T) washes, and blocking (TBS-T, 5% nonfat milk powder for 1 h), the membranes were reprobed for evidence of Rab7 using the same method. The relative amounts of RILP and Rab7 in each preparation were quantified using Quantity-1 densitometry software and used to calculate the proportion of RILP to Rab7 in each bacterial treatment.

Secondary *E. coli* infection. Monocytes (2×10^5) were preincubated with mycobacteria (MOI, 50:1) for 2 h before the addition of *E. coli* (strain BL21 or LF82; MOI, 20:1) for 2 h and then gentamicin (final concentration 100 μg/ml) for a further 2 h to kill extracellular bacteria. Intracellular *E. coli* was retrieved from infected cells using 0.1% Triton X-100 in PBS for 10 min at 37°C to give cell lysates that were serially diluted (in PBS) and cultured (in duplicate) on sheep blood agar plates (Fort Richard, Auckland, New Zealand) overnight for CFU determinations.

Statistical analysis. Results are the means ± standard errors of the means (SEMs). Data were analyzed by one-way or repeated-measures analysis of variance (ANOVA). If the ANOVA P value was <0.05, this was followed by Dunnett's *post hoc* test.

RESULTS

Cholesterol accumulates at the site of *M. avium* subsp. *paratuberculosis* entry into THP-1 cells. An association between the uptake of *M. avium* subsp. *paratuberculosis* and the distribution of plasma membrane-associated cholesterol was visualized in human monocyte THP-1 cells by fluorescence microscopy. Filipin, which binds cholesterol in mammalian cells (9), revealed the homogeneous distribution of this sterol in the plasma membrane of

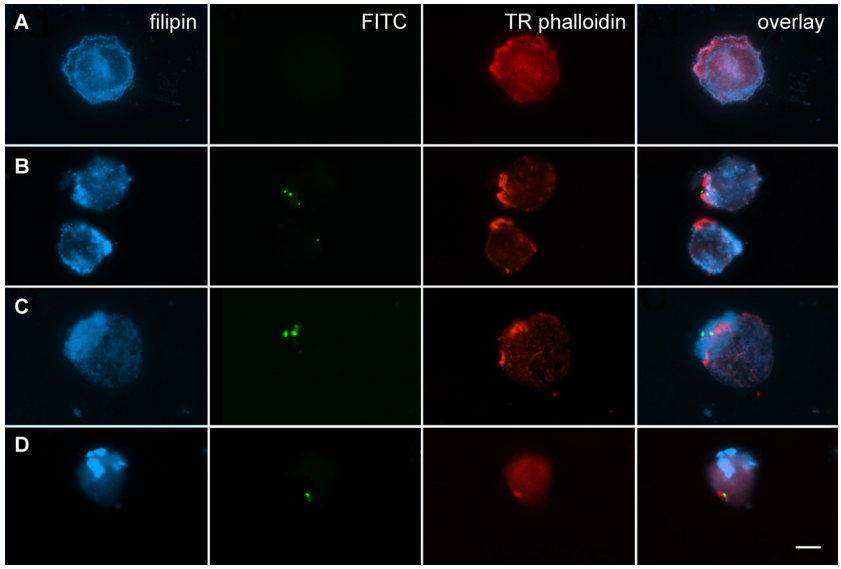

FIG 1 Cholesterol aggregates at the site of *M. avium* subsp. *paratuberculosis* internalization. THP-1 cells infected with bacteria (MOI, 50:1) for 4 h were fixed, stained, and visualized for filipin-labeled cholesterol, FITC-labeled bacteria, and Texas Red-conjugated phalloidin-stained actin. The right-hand column shows an overlay image. The images, which are representative of three independent experiments, denote cells with no bacteria (A), *M. bovis* (B), *M. avium* subsp. *paratuberculosis* (C), and *E. coli* BL21 (D). Bar = 10 μm.

untreated cells (Fig. 1A), as well as some aggregation not always specific to areas of bacterial uptake in infected cells (Fig. 1B to D). An accumulation of cholesterol was observed at the site of *M. avium* subsp. *paratuberculosis* (Fig. 1B) and *M. bovis* (Fig. 1C) internalization into THP-1 cells after 4 h of incubation. In contrast, *E. coli* BL21 entry into the cells occurred without any evidence of cholesterol accumulation (Fig. 1D).

Depletion of cellular cholesterol decreases uptake of *M. avium* subsp. *paratuberculosis* into THP-1 cells. To investigate the association between *M. avium* subsp. *paratuberculosis* and cholesterol, THP-1 cells were treated with the cholesterol-reducing drug simvastatin and the cholesterol chelator MβCD, used in tandem at concentrations of 2.5 μg/ml and up to 5 mM, respectively (12). Simvastatin caused a decrease in cholesterol to 1.36 ± 0.25 μg/mg protein from the 1.63 ± 0.24 μg/mg protein in untreated cells, while simvastatin and 5 μM MβCD reduced cholesterol even further to 1.08 ± 0.27 μg/mg protein (Fig. 2A). These drugs had no effect on cell proliferation or viability (not shown), and cholesterol levels returned to normal when MβCD complexed with cholesterol was added to simvastatin-treated cells (Fig. 2A). Using cells with reduced cholesterol, in conjunction with flow cytometry, we found that pretreatment of simvastatin-treated cells with 5 mM MβCD significantly inhibited the internalization of labeled *M. avium* subsp. *paratuberculosis* (Fig. 2B) and *M. bovis* (Fig. 2C) bacteria ($P < 0.05$ and 0.01, respectively). In contrast, *E. coli* BL21 internalization was unaffected (Fig. 2D).

***M. avium* subsp. *paratuberculosis* resides in cholesterol-rich compartments inside monocytes.** As cholesterol-dependent uptake of *M. avium* subsp. *paratuberculosis* need not imply ongoing involvement of cholesterol in the intracellular trafficking of these bacteria, we used fluorescence microscopy of living cells to determine whether those compartments that contained *M. avium* subsp. *paratuberculosis* maintained high levels of cholesterol after internalization. Filipin staining of THP-1 cells at 48 h postinfection identified that all intracellular FITC-labeled *M. avium* subsp. *paratuberculosis* bacteria were colocalized with cholesterol (Fig. 3). Additionally, cholesterol formed a cloud around the bacteria when a 3-dimensional model of this *M. avium* subsp. *paratuberculosis*-containing phagosome was constructed (see Movie S1 in the supplemental material), similar to that observed around other pathogenic bacteria in intracellular compartments (3). Together, these findings suggest an ongoing association between *M. avium* subsp. *paratuberculosis* and cholesterol that may contribute to bacterial persistence.

***M. avium* subsp. *paratuberculosis* colocalizes with Rab7.** THP-1 cells infected with *M. avium* subsp. *paratuberculosis* for 2 h were probed with antibodies against Rab5a (one of three isoforms of Rab5) and Rab7, two small GTPases that are characteristic of the binding of early and late endosomal compartments to the phagosome, respectively (41). We failed to detect Rab5a staining in any cells, including uninfected controls (not shown). In contrast, Rab7 was detected in most bacterium-containing compartments (including those containing *E. coli* BL21) after 2 h of infection (Fig. 4). Additionally, the mycobacterium-containing phagosomes retained this marker to 48 h postinfection, with no significant difference seen between live and killed mycobacterial preparations, whereas *E. coli* was cleared from the cells by this time (not shown).

Compartments containing live *M. avium* subsp. *paratuberculosis* are less acidic. Rab7 recruitment to phagosomes occurs before the final step in phagosomal maturation, which involves binding and fusion of secondary lysosomes and subsequent acidification of the phagosome (41). The enumeration (by microscopy) of *M. avium* subsp. *paratuberculosis*-containing compartments after staining with LysoTracker Red, a fluorophore with a weak base attached that is highly selective for acidic organelles, confirmed that compartments that contained live *M. avium* subsp. *paratuberculosis* bacteria were notably less acidic than those compartments that contained heat-killed bacteria (Fig. 5).

***M. avium* subsp. *paratuberculosis*-containing phagosomes exhibit impaired RILP acquisition.** Recent studies report that, despite normal acquisition of Rab7, mycobacterial pathogens

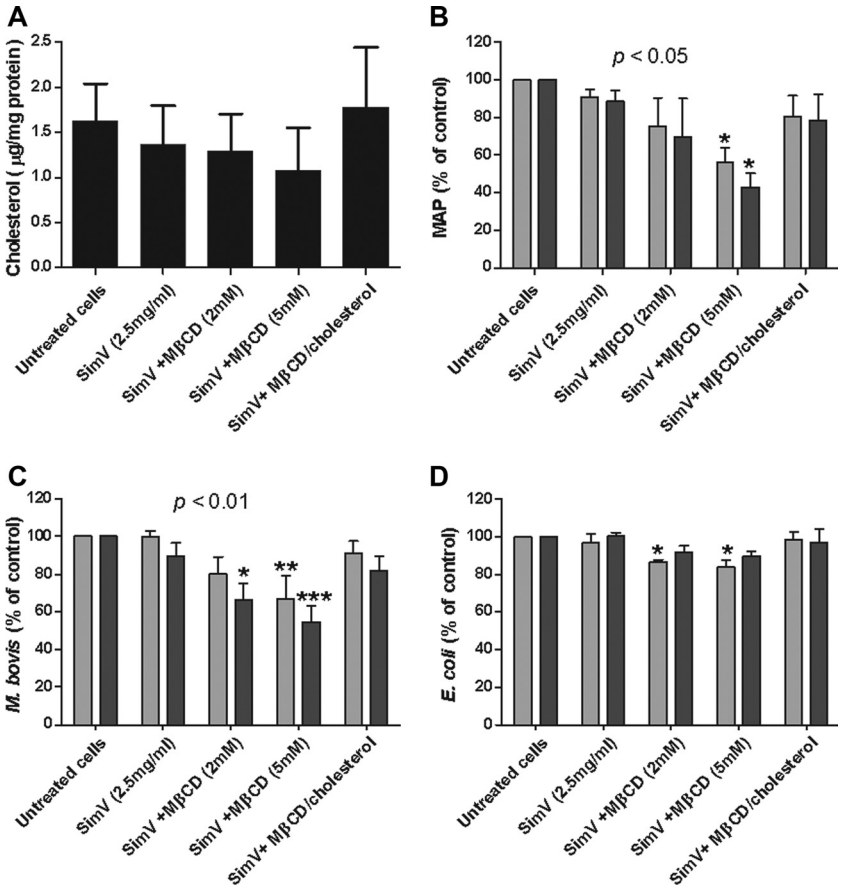

FIG 2 Flow cytometry assessment of internalization of labeled bacteria into cholesterol-depleted THP-1 cells. (A) A negative cholesterol gradient was created in THP-1 cells using simvastatin (SimV) and MβCD. Cells were incubated with FITC-labeled *M. avium* subsp. *paratuberculosis* (MAP) (B), *M. bovis* (C), or *E. coli* BL21 (D) (all at an MOI of 50:1) for 4 h, and then fluorescence was measured before (total associated; light bars) and after (intracellular; dark bars) the addition of trypan blue. Lowering cholesterol had a significant effect on the internalization of *M. avium* subsp. *paratuberculosis* and *M. bovis* ($P < 0.05$ and 0.01, respectively). *, **, and ***, results are statistically significantly different from those for untreated controls ($P < 0.05$, 0.01, and 0.001, respectively). Results are ±SEMs for three independent experiments.

such as *M. tuberculosis* and *M. bovis* secrete on the phagosomal membrane a factor that inactivates Rab7, rendering it unable to recruit its effector protein, RILP. This in turn precludes fusion of these phagosomes with lysosomes (38, 39). We observed that the infection with live *M. avium* subsp. *paratuberculosis* or *M. bovis* was associated with a reduced recruitment of RILP (Fig. 6B) relative to Rab7 (Fig. 6A) in phagosomes isolated from THP-1 cells at 48 h postinfection. Phagosomal recruitment of RILP was significantly more evident in the phagosomes of THP-1 cells infected with heat-killed *M. avium* subsp. *paratuberculosis* (Fig. 6C). These results suggest that the recruitment of RILP by Rab7 on the phagosomal membrane is interrupted in phagosomes of live *M. avium* subsp. *paratuberculosis*-containing cells, as seen in *M. bovis*-containing phagosomes.

Preincubation of THP-1 cells with live *M. avium* subsp. *paratuberculosis* fails to facilitate *E. coli* persistence. A recent study

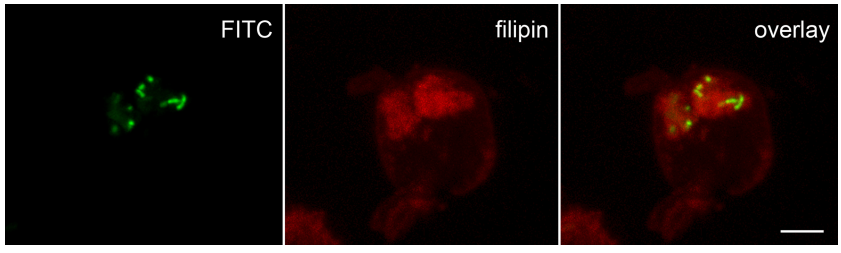

FIG 3 Intracellular *M. avium* subsp. *paratuberculosis* colocalizes with cholesterol. THP-1 cells infected with FITC-labeled bacteria (MOI, 50:1) for 48 h were examined using a ×40 oil-immersion (numerical aperture, 1.3) lens and confocal microscopy (model SP5; Leica, Wetzlar, Germany). Filipin, indicated in red, was excited with 405 nm light (violet), and emission was collected from 420 to 480 nm, while FITC, shown in green, was excited with 488 nm (blue) light and fluorescence was collected from 500 to 550 nm. Bar = 5 μm.

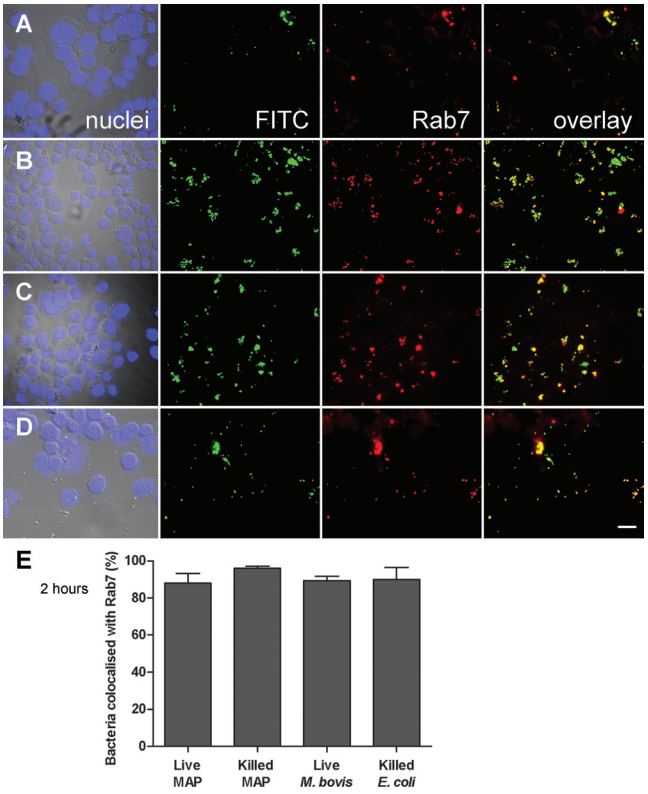

FIG 4 Colocalization of Rab7 with *M. avium* subsp. *paratuberculosis*. Epifluorescence images of FITC-labeled live (A) and heat-killed (B) *M. avium* subsp. *paratuberculosis*, live *M. bovis* (C), and heat-killed *E. coli* BL21 (D) at 2 h postinfection of THP-1 cells (MOI, 50:1). Blue nuclei, green bacteria, and red Rab7 fluorescence are shown individually and in a merged image. Bar = 20 μm. (E) Mean ± SEM bacterial colocalization with Rab7 (yellow fluorescence) in 150 bacterium-containing phagosomes from three independent experiments.

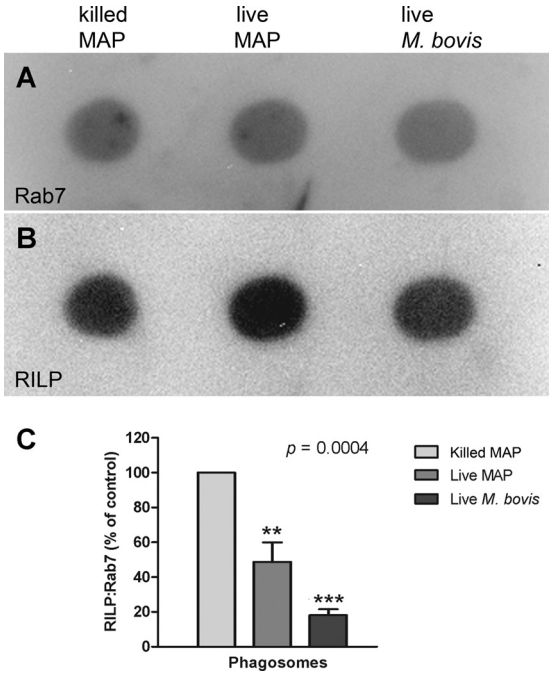

FIG 6 Live *M. avium* subsp. *paratuberculosis* reduces phagosomal recruitment of RILP. At 48 h postinfection, bacterium-containing phagosomes were isolated from infected THP-1 cells by sucrose density gradient centrifugation. Phagosome preparations were dot blotted onto a PVDF membrane and probed first with an anti-RILP antibody. Bound antibody was removed with glycine-HCl, and the blot was reprobed with an antibody to Rab7. Antibody binding to RILP (A) and Rab7 (B) was visualized using an alkaline phosphatase-conjugated secondary antibody and quantified using densitometry. The ratio of RILP/Rab7 was calculated and is shown normalized (C) to that for heat-killed *M. avium* subsp. *paratuberculosis* (100%). Overall, at 48 h cells infected with live mycobacteria (both *M. avium* subsp. *paratuberculosis* and *M. bovis*) had significantly reduced expression of RILP relative to expression of Rab7 in phagosome preparations ($P = 0.0004$). ** and ***, results are significantly different from those for THP-1 cells infected with heat-killed *M. avium* subsp. *paratuberculosis* ($P < 0.01$ and 0.001, respectively). Results are ±SEMs for three independent experiments.

showed that a factor secreted by pathogenic *M. bovis* can diffuse out of the phagosome and modify GTPase activity in other phagosomal compartments (39). Given the reduced recruitment of RILP to phagosomes from *M. avium* subsp. *paratuberculosis*-infected cells, we investigated whether the presence of live *M. avium* subsp. *paratuberculosis* inside monocytes could decrease the killing efficiency of these cells when presented with a second bacterial challenge. For these experiments, we used both THP-1 cells and freshly isolated human monocytes that were challenged with two strains of *E. coli*, including strain LF82, which is associated with CD (15). Pretreatment of THP-1 cells with live *M. avium* subsp. *paratuberculosis* increased the uptake of both strains of *E. coli*,

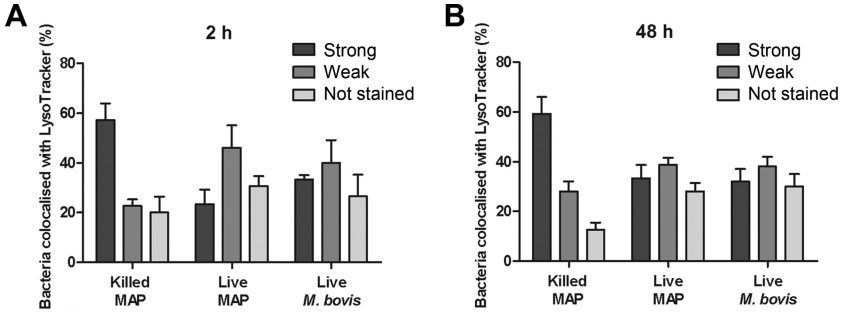

FIG 5 Live *M. avium* subsp. *paratuberculosis* exhibits altered fusion with acidic compartments. THP-1 cells were infected with FITC-labeled *M. avium* subsp. *paratuberculosis* (MOI, 50:1) and labeled with LysoTracker Red, and using a merged image, bacterium-containing compartments were counted manually as strongly, weakly, or not stained with LysoTracker Red. Values are the means ± SEMs of live *M. avium* subsp. *paratuberculosis* colocalization with LysoTracker Red in 150 bacterium-containing compartments from three independent experiment compared to those for heat-killed *M. avium* subsp. *paratuberculosis* and live *M. bovis*.

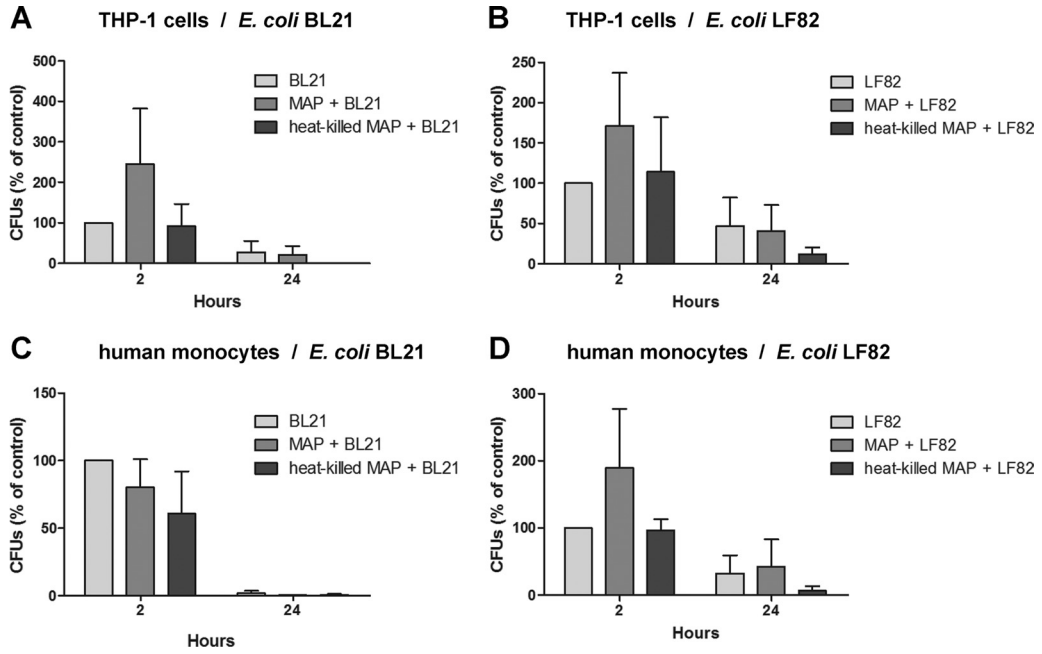

FIG 7 Secondary *E. coli* infection of human monocytes after primary infection with *M. avium* subsp. *paratuberculosis*. *E. coli* bacteria (MOI, 20:1) added to cells 2 h after infection with *M. avium* subsp. *paratuberculosis* (MOI, 50:1) were given 2 h to internalize before the addition of gentamicin to kill any remaining extracellular bacteria. Quantitative assessment of viable *E. coli* in THP-1 cells (A and B) and purified human monocytes (C and D) 2 and 24 h after coinfection was by serial dilution of cell lysates. Results are ±SEMs for three independent experiments.

evidenced by an increase in the number of *E. coli* CFU recovered from the lysed cells at 2 h postinfection. However, a similar trend was not observed when freshly isolated human monocytes were incubated with the BL21 strain of *E. coli*, and importantly, these differences were not sustained in either cell type over time. Notably fewer *E. coli* CFU were recovered from the cells after 24 h of incubation, irrespective of prior *M. avium* subsp. *paratuberculosis* challenge (Fig. 7). Collectively, these results suggest that internalized *M. avium* subsp. *paratuberculosis* is unlikely to affect the survival of bacteria taken up during a secondary phagocytic event.

DISCUSSION

Our interest in *M. avium* subsp. *paratuberculosis* as a potential human pathogen stems from the high incidence of CD in our community, the Canterbury region of New Zealand (13), and the correspondingly high number of these patients who have evidence of the *M. avium* subsp. *paratuberculosis*-specific DNA insertion sequence IS*900* in their blood and tissues (2). Manipulation of the phagocytic pathway is a hallmark of intracellular bacterial pathogens, and a number of mycobacterial species are included in the growing list of pathogenic bacteria that exploit lipid-rich domains to invade and persist within human cells (46). Added to this is an observation of *M. avium* subsp. *paratuberculosis* survival in polymorphonuclear leukocytes, which supports the hypothesis that *M. avium* subsp. *paratuberculosis* may be a human pathogen (33).

We observed that *M. avium* subsp. *paratuberculosis* associates with and is internalized into THP-1 monocytes in a cholesterol-dependent manner and at cholesterol-rich areas of the membrane. This, coupled with our finding of cholesterol-dependent *M. bovis* uptake by THP-1 cells, is consistent with other studies of pathogenic mycobacteria (12, 22, 32). Intriguingly, significantly fewer *E. coli* bacteria associated with cells as cellular cholesterol levels fell. However, *E. coli* internalization was not significantly affected by lowered cholesterol levels, suggesting that these bacteria are internalized into cells via a cholesterol-independent mechanism (12).

There is evidence that cholesterol-rich membrane microdomains (lipid rafts) act as receptor-mediated signaling platforms (24), as well as portals for bacterial uptake (27). The association with cholesterol-rich compartments inside cells may reflect the ability of pathogenic mycobacteria to use the cholesterol as a supplemental carbon source, enabling them to remain metabolically active (30). In addition, cellular cholesterol may actively affect processes associated with normal bacterial clearance. One example is the cholesterol-dependent binding of the mycobacterial protein lipoamide dehydrogenase C (LpdC) to coronin-1 (also known as TACO) on the phagosomal membrane (10, 12, 22). Binding aids retention of the coronin-1 protein (8), which, in turn, facilitates phagosome maturation arrest (10) by blocking lysosomal delivery (21). We found evidence of coronin-1 protein in approximately 40% of *M. avium* subsp. *paratuberculosis*-infected THP-1 cells at 48 h postinfection (D. A. Keown, unpublished data). However, coronin-1 was also retained on phagosomes containing heat-killed bacteria. The reason for this is currently unknown.

The rapid recruitment of Rab7 identified the *M. avium* subsp. *paratuberculosis*-containing compartments as late phagosomes. However, the compartments containing live bacteria acidified less readily over time than those containing killed bacteria, suggesting that whereas Rab7 recruitment might be a precursor, it was not necessarily sufficient to promote the maturation of late phagosomes to phagolysosomes (41). Rab7 is recruited to the phagosomal membrane when activated, where it interacts with an effector protein (RILP), initiating a process that leads to the recruitment and fusion of lysosomes with the late phagosomal compartment (18, 41).

We found that phagosomes from THP-1 cells infected with live *M. avium* subsp. *paratuberculosis* bacteria failed to recruit RILP as efficiently as those containing dead bacteria, despite the presence of Rab7. *M.* bovis (38) and *M. tuberculosis* (25) also interfere with RILP recruitment to active Rab7 in bacterium-containing compartments, and there is evidence to suggest that this may be due to the action of bacterial factors.

Live *M. bovis* bacteria secrete a protein that is capable of inactivating Rab7, thus rendering it unable to recruit RILP (38). This protein, recently identified as nucleotide diphosphate kinase (NDK), is also considered a putative *M. tuberculosis* virulence factor (39). The reported diffusibility of this protein (38) and corresponding ability to reduce GTPase activity on other phagosomal compartments within the cell (39) led us to investigate whether the presence of *M. avium* subsp. *paratuberculosis* might affect the clearance of *E. coli* taken up in a secondary phagocytic event. We observed that prior infection of THP-1 cells with live *M. avium* subsp. *paratuberculosis* generally led to enhanced *E. coli* phagocytosis. This may reflect changes to the intracellular environment of infected cells, as reported following *M. avium* subsp. *paratuberculosis* invasion of bovine epithelial cells (31). However, unlike Hart el al., who showed that pretreatment with live but not dead *M. microti* bacteria for 18 to 24 h before challenge with *Saccharomyces cerevisiae* significantly inhibited the fusion of yeast-containing phagosomes with lysosomes (19), we found no evidence that pretreatment of human monocytes with *M. avium* subsp. *paratuberculosis* affected the survival of *E. coli.* Our failure to replicate the study of Hart et al. (19) may, in part, reflect our use of a different mycobacterial species and bacterial rather than fungal secondary challenge and/or differences between human monocytic cells and murine macrophages.

In summary, we have shown that *M. avium* subsp. *paratuberculosis* utilizes cholesterol to enter and persist in human cells inside compartments that acidify inefficiently compared with those containing killed bacteria. We propose that this is brought about by the ineffective recruitment of RILP to the phagosomal membrane, possibly enhanced by the retention of cholesterol in these compartments. It remains to be determined if this is linked to *M. avium* subsp. *paratuberculosis* secretion of proteins such as LpdC and/or Ndk or, indeed, if these apparently disparate mechanisms are linked. In addition, further research will be necessary before we can conclude that the apparent manipulation of phagosome maturation by *M. avium* subsp. *paratuberculosis* is sufficient to contribute to disease processes in human cells associated with CD.

ACKNOWLEDGMENTS

We thank Kenny Chitcholtan for his assistance with microscopy, Robert Bentley and Amy Scott-Thomas for their generous gifts of mycobacterial strains, and Peter Tyrer, Kelly Jones, and Nina Salm for their invaluable technical assistance and critical analysis.

This work was partially supported by a grant from the Canterbury Bowel and Liver Trust.

REFERENCES

1. **Autschbach F, et al.** 2005. High prevalence of *Mycobacterium avium* subspecies *paratuberculosis* IS900 DNA in gut tissues from individuals with Crohn's disease. Gut **54**:944–949.
2. **Bentley RW, et al.** 2008. Incidence of *Mycobacterium avium* subspecies *paratuberculosis* in a population-based cohort of patients with Crohn's disease and control subjects. Am. J. Gastroenterol. **103**:1168–1172.
3. **Catron DM, et al.** 2004. *Salmonella enterica* serovar *Typhimurium* requires nonsterol precursors of the cholesterol biosynthetic pathway for intracellular proliferation. Infect. Immun. **72**:1036–1042.
4. **Cheville NF, et al.** 2001. Intracellular trafficking of *Mycobacterium avium ss. paratuberculosis* in macrophages. Dtsch. Tierarztl. Wochenschr. **108**: 236–243.
5. **Chiodini RJ.** 1989. Crohn's disease and the mycobacterioses: a review and comparison of two disease entities. Clin. Microbiol. Rev. **2**:90–117.
6. **Clemens DL, Lee BY, Horwitz MA.** 2000. *Mycobacterium tuberculosis* and *Legionella pneumophila* phagosomes exhibit arrested maturation despite acquisition of Rab7. Infect. Immun. **68**:5154–5166.
7. **de Chastellier C, Thilo L.** 2006. Cholesterol depletion in *Mycobacterium avium*-infected macrophages overcomes the block in phagosome maturation and leads to the reversible sequestration of viable mycobacteria in phagolysosome-derived autophagic vacuoles. Cell. Microbiol. **8**:242–256.
8. **Deghmane AE, et al.** 2007. Lipoamide dehydrogenase mediates retention of coronin-1 on BCG vacuoles, leading to arrest in phagosome maturation. J. Cell Sci. **120**:2796–2806.
9. **Drabikowski W, Lagwinska E, Sarzala MG.** 1973. Filipin as a fluorescent probe for the location of cholesterol in the membranes of fragmented sarcoplasmic reticulum. Biochim. Biophys. Acta **291**:61–70.
10. **Ferrari G, Langen H, Naito M, Pieters J.** 1999. A coat protein on phagosomes involved in the intracellular survival of mycobacteria. Cell **97**:435–447.
11. **Fratti RA, Chua J, Deretic V.** 2003. Induction of p38 mitogen-activated protein kinase reduces early endosome autoantigen 1 (EEA1) recruitment to phagosomal membranes. J. Biol. Chem. **278**:46961–46967.
12. **Gatfield J, Pieters J.** 2000. Essential role for cholesterol in entry of mycobacteria into macrophages. Science **288**:1647–1650.
13. **Gearry RB, et al.** 2006. High incidence of Crohn's disease in Canterbury, New Zealand: results of an epidemiologic study. Inflamm. Bowel Dis. **12**:936–943.
14. **Geijtenbeek TB, et al.** 2003. Mycobacteria target DC-SIGN to suppress dendritic cell function. J. Exp. Med. **197**:7–17.
15. **Glasser AL, et al.** 2001. Adherent invasive *Escherichia coli* strains from patients with Crohn's disease survive and replicate within macrophages without inducing host cell death. Infect. Immun. **69**:5529–5537.
16. **Glubb DM, et al.** 2011. NOD2 and ATG16L1 polymorphisms affect monocyte responses in Crohn's disease. World J. Gastroenterol. **17**:2829–2837.
17. **Goswami T, Joardar S, Ram G, Banerjee R, Singh D.** 2000. Association of *Mycobacterium paratuberculosis* in Crohn's disease and Johne's disease: a possible zoonotic threat. Curr. Sci. **79**:1076–1081.
18. **Harrison RE, Bucci C, Vieira OV, Schroer TA, Grinstein S.** 2003. Phagosomes fuse with late endosomes and/or lysosomes by extension of membrane protrusions along microtubules: role of Rab7 and RILP. Mol. Cell. Biol. **23**:6494–6506.
19. **Hart PD, Young MR, Gordon AH, Sullivan KH.** 1987. Inhibition of phagosome-lysosome fusion in macrophages by certain mycobacteria can be explained by inhibition of lysosomal movements observed after phagocytosis. J. Exp. Med. **166**:933–946.
20. **Huynh KK, Gershenzon E, Grinstein S.** 2008. Cholesterol accumulation by macrophages impairs phagosome maturation. J. Biol. Chem. **283**: 35745–35755.
21. **Jayachandran R, et al.** 2007. Survival of mycobacteria in macrophages is mediated by coronin 1-dependent activation of calcineurin. Cell **130**:37–50.
22. **Kaul D, Anand PK, Verma I.** 2004. Cholesterol-sensor initiates *M. tuberculosis* entry into human macrophages. Mol. Cell. Biochem. **258**:219–222.
23. **Kuehnel MP, et al.** 2001. Characterization of the intracellular survival of *Mycobacterium avium ssp. paratuberculosis*: phagosomal pH and fusogenicity in J774 macrophages compared with other mycobacteria. Cell. Microbiol. **3**:551–566.
24. **Lafont F, van der Goot FG.** 2005. Bacterial invasion via lipid rafts. Cell. Microbiol. **7**:613–620.
25. **Lee BY, Clemens DL, Horwitz MA.** 2008. The metabolic activity of *Mycobacterium tuberculosis*, assessed by use of a novel inducible GFP expression system, correlates with its capacity to inhibit phagosomal maturation and acidification in human macrophages. Mol. Microbiol. **68**: 1047–1060.
26. **Luhrmann A, Haas A.** 2000. A method to purify bacteria-containing phagosomes from infected macrophages. Methods Cell Sci. **22**:329–341.

27. **Manes S, del Real G, Martinez AC.** 2003. Pathogens: raft hijackers. Nat. Rev. Immunol. **3**:557–568.
28. **Naser SA, Ghobrial G, Romero C, Valentine JF.** 2004. Culture of *Mycobacterium avium* subspecies *paratuberculosis* from the blood of patients with Crohn's disease. Lancet **364**:1039–1044.
29. **Olsen I, et al.** 2009. Isolation of *Mycobacterium avium* subspecies *paratuberculosis* reactive CD4 T cells from intestinal biopsies of Crohn's disease patients. PLoS One **4**:e5641. doi:10.1371/journal.pone.0005641.
30. **Pandey AK, Sassetti CM.** 2008. Mycobacterial persistence requires the utilization of host cholesterol. Proc. Natl. Acad. Sci. U. S. A. **105**:4376–4380.
31. **Patel D, et al.** 2006. The ability of *Mycobacterium avium* subsp. *paratuberculosis* to enter bovine epithelial cells is influenced by preexposure to a hyperosmolar environment and intracellular passage in bovine mammary epithelial cells. Infect. Immun. **74**:2849–2855.
32. **Peyron P, Bordier C, N′Diaye EN, Maridonneau-Parini I.** 2000. Nonopsonic phagocytosis of *Mycobacterium kansasii* by human neutrophils depends on cholesterol and is mediated by CR3 associated with glycosylphosphatidylinositol-anchored proteins. J. Immunol. **165**:5186–5191.
33. **Rumsey J, Valentine JF, Naser SA.** 2006. Inhibition of phagosome maturation and survival of *Mycobacterium avium* subspecies *paratuberculosis* in polymorphonuclear leukocytes from Crohn's disease patients. Med. Sci. Monit **12**:BR130–BR139.
34. **Sandermann H, Jr, Strominger JL.** 1972. Purification and properties of C 55-isoprenoid alcohol phosphokinase from *Staphylococcus aureus.* J. Biol. Chem. **247**:5123–5131.
35. **Singh AV, Singh SV, Singh PK, Sohal JS.** 2010. Is *Mycobacterium avium* subsp. *paratuberculosis*, the cause of Johne's disease in animals, a good candidate for Crohn's disease in man? Indian J. Gastroenterol. **29**:53–58.
36. **Souza CD, Evanson OA, Sreevatsan S, Weiss DJ.** 2007. Cell membrane receptors on bovine mononuclear phagocytes involved in phagocytosis of *Mycobacterium avium* subsp *paratuberculosis.* Am. J. Vet. Res. **68**:975–980.
37. **Souza CD, Evanson OA, Weiss DJ.** 2007. Role of the mitogen-activated protein kinase pathway in the differential response of bovine monocytes to *Mycobacterium avium* subsp. *paratuberculosis* and *Mycobacterium avium* subsp. *avium.* Microbes Infect. **9**:1545–1552.
38. **Sun J, et al.** 2007. *Mycobacterium bovis* BCG disrupts the interaction of Rab7 with RILP contributing to inhibition of phagosome maturation. J. Leukoc. Biol. **82**:1437–1445.
39. **Sun J, et al.** 2010. Mycobacterial nucleoside diphosphate kinase blocks phagosome maturation in murine RAW 264.7 macrophages. PLoS One **5**:e8769. doi:10.1371/journal.pone.0008769.
40. **Via LE, et al.** 1997. Arrest of mycobacterial phagosome maturation is caused by a block in vesicle fusion between stages controlled by rab5 and rab7. J. Biol. Chem. **272**:13326–13331.
41. **Vieira OV, Botelho RJ, Grinstein S.** 2002. Phagosome maturation: aging gracefully. Biochem. J. **366**:689–704.
42. **Weiss DJ, Souza CD, Evanson OA, Sanders M, Rutherford M.** 2008. Bovine monocyte TLR2 receptors differentially regulate the intracellular fate of *Mycobacterium avium* subsp. *paratuberculosis* and *Mycobacterium avium* subsp. *avium.* J. Leukoc. Biol. **83**:48–55.
43. **Woo SR, Heintz JA, Albrecht R, Barletta RG, Czuprynski CJ.** 2007. Life and death in bovine monocytes: the fate of *Mycobacterium avium* subsp. *paratuberculosis.* Microb. Pathog. **43**:106–113.
44. **Woo SR, Sotos J, Hart AP, Barletta RG, Czuprynski CJ.** 2006. Bovine monocytes and a macrophage cell line differ in their ability to phagocytose and support the intracellular survival of *Mycobacterium avium* subsp. *paratuberculosis.* Vet. Immunol. Immunopathol. **110**:109–120.
45. **Wooldridge KG, Williams PH, Ketley JM.** 1996. Host signal transduction and endocytosis of *Campylobacter jejuni.* Microb. Pathog. **21**:299–305.
46. **Zaas DW, Duncan M, Rae Wright J, Abraham SN.** 2005. The role of lipid rafts in the pathogenesis of bacterial infections. Biochim. Biophys. Acta **1746**:305–313.